

Endothelium-Restricted Overexpression of Human Endothelin-1 Causes Vascular Remodeling and Endothelial Dysfunction

Farhad Amiri, PhD; Agostino Viridis, MD; Mario Fritsch Neves, MD; Marc Iglarz, PharmD, PhD;
Nabil G. Seidah, PhD; Rhian M. Touyz, MD, PhD;
Timothy L. Reudelhuber, PhD; Ernesto L. Schiffrin, MD, PhD, FRCPC

Background—Endothelin (ET)-1 is a potent vasoconstrictor that contributes to vascular remodeling in hypertension and other cardiovascular diseases. Endogenous ET-1 is produced predominantly by vascular endothelial cells. To directly test the role of endothelium-derived ET-1 in cardiovascular pathophysiology, we specifically targeted expression of the human preproET-1 gene to the endothelium by using the Tie-2 promoter in C57BL/6 mice.

Methods and Results—Ten-week-old male C57BL/6 transgenic (TG) and nontransgenic (wild type; WT) littermates were studied. TG mice exhibited 3-fold higher vascular tissue ET-1 mRNA and 7-fold higher ET-1 plasma levels than did WT mice but no significant elevation in blood pressure. Despite the absence of significant blood pressure elevation, TG mice exhibited marked hypertrophic remodeling and oxidant excess–dependent endothelial dysfunction of resistance vessels, altered ET-1 and ET-3 vascular responses, and significant increases in ET_B expression compared with WT littermates. Moreover, TG mice generated significantly higher oxidative stress, possibly through increased activity and expression of vascular NAD(P)H oxidase than did their WT counterparts.

Conclusions—In this new murine model of endothelium-restricted human preproET-1 overexpression, ET-1 caused structural remodeling and endothelial dysfunction of resistance vessels, consistent with a direct nonhemodynamic effect of ET-1 on the vasculature, at least in part through the activation of vascular NAD(P)H oxidase. (*Circulation*. 2004;110:2233-2240.)

Key Words: endothelin ■ remodeling ■ cardiovascular diseases ■ endothelium ■ free radicals

Vascular remodeling plays an important role in the pathophysiology of hypertension and cardiovascular disease, and endothelin (ET)-1 may be involved in this process.¹ ET-1, a potent vasoconstrictor produced primarily by the endothelium of blood vessels,² can act in either a paracrine or an autocrine manner³ via ET type A (ET_A) or ET type B (ET_B) receptors on adjacent endothelial and smooth muscle cells, which are coupled to an array of signaling pathways.⁴ The role of ET-1 in hypertension was initially observed in models of experimental hypertension, such as the deoxycorticosterone acetate (DOCA)–salt hypertensive, Dahl salt-sensitive, and stroke-prone spontaneously hypertensive rat strains, in which ET-1 induced vascular hypertrophy and blood pressure (BP) elevation.^{1,5} More recently, generation of specific knockouts of the different components of the ET-1 system^{6–11} and human ET-1 transgenic (TG) models^{12,13} have confirmed the importance of ET-1 in vascular disease. Collectively, these data have strongly suggested that activation of vascular ET-1 is associated with growth and proinflammatory effects and the remodeling of resistance arteries^{14,15} through

several mechanisms, including increased oxidative stress.^{16,17} Several types of vascular remodeling exist,¹⁸ which may be associated with media growth (hypertrophic remodeling) or devoid of media growth (eutrophic remodeling),¹⁹ and depend on changes in the expression of properties of adhesion molecules or a combination of inward growth and outer apoptosis, leading to a decrease in the outer and inner diameters of vessels.²⁰ We previously suggested that experimental models of hypertension that exhibit hypertrophic remodeling involve the participation of ET-1 in the growth process.^{1,5,14,15,21} In addition, it has been suggested that ET-1 is implicated in the development of vascular changes through the generation of reactive oxygen species (ROS) through NAD(P)H oxidase activation.^{17,22,23} However, in existing models of hypertension, the expression of ET-1 is associated with other mechanisms that are activated, and the direct cellular effects of ET-1 cannot be distinguished from those of these other agents. Thus, the primary role of ET-1 produced by the endothelium remains to be elucidated. To address this question, we generated TG mice overexpressing human

Received September 18, 2003; de novo received January 29, 2004; revision received May 20, 2004; accepted May 21, 2004.

From the Experimental Hypertension (F.A., A.V., M.F.N., M.I., R.M.T., E.L.S.) and Molecular Biochemistry of Hypertension (T.L.R.) Laboratories of the CIHR Multidisciplinary Research Group on Hypertension, and the Laboratory of Biochemical Neuroendocrinology (N.G.S.), Clinical Research Institute of Montreal, Montreal, Canada.

Correspondence to Ernesto L. Schiffrin, MD, PhD, FRCPC, Clinical Research Institute of Montreal, 110 Pine Ave W, Montreal, Quebec, Canada H2W 1R7. E-mail ernesto.schiffrin@ircm.qc.ca

© 2004 American Heart Association, Inc.

Circulation is available at <http://www.circulationaha.org>

DOI: 10.1161/01.CIR.0000144462.08345.B9

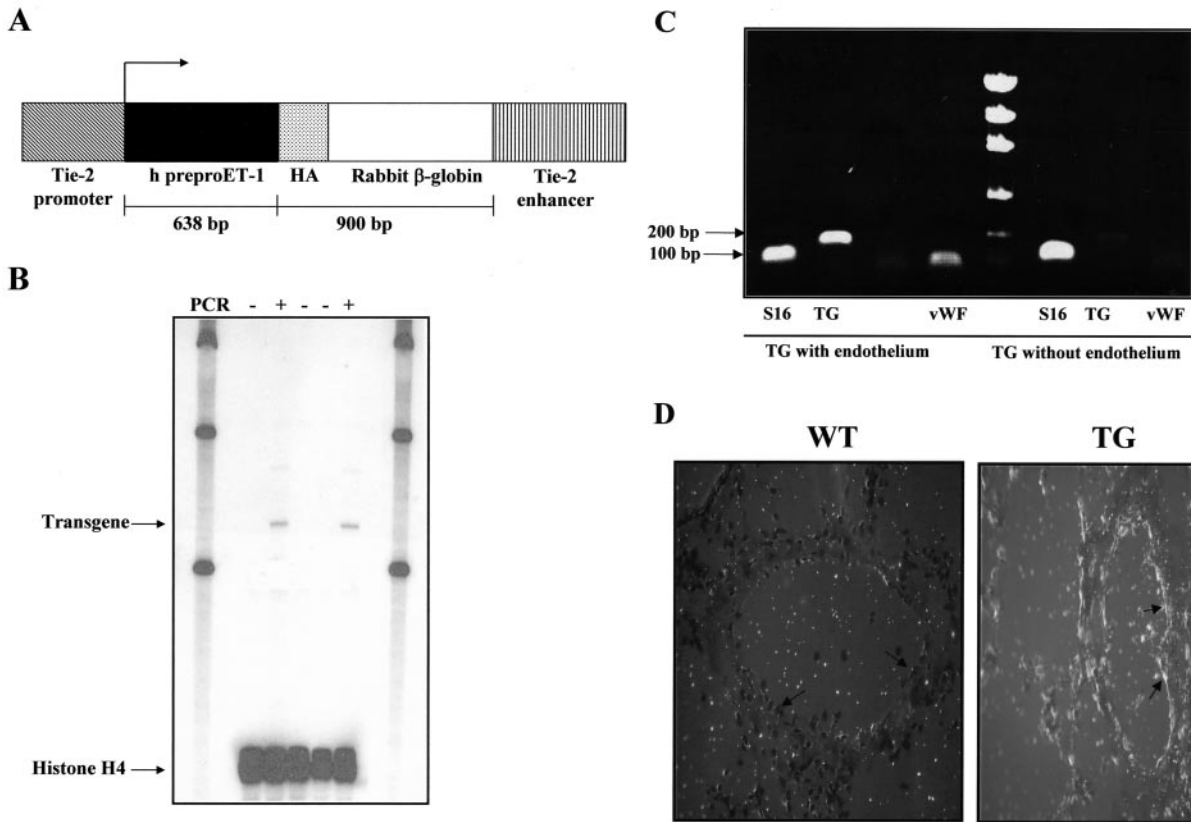


Figure 1. Endothelium targeting of human preproET-1 gene. A, Human preproET-1 TG diagram, where HA represents hemagglutinin. See Methods for details. B, RPA confirming TG expression. +/- Refers to TG presence/absence as determined by PCR of tail biopsy DNA. C, TG localization as confirmed by RT-PCR for vWF and S16. D, Distribution of TG expression in lung vessels determined by in situ hybridization. Arrows denote endothelial cells. Magnification 40 \times . All other abbreviations are as defined in text.

preproET-1 specifically in blood vessel endothelium by using the endothelium-specific promoter Tie-2.²⁴ Using this new TG model, we have investigated the role of endothelium-generated ET-1 on the endothelial function and vascular structure of small resistance arteries.

Methods

Endothelium Targeting of Human PreproET-1 Gene

To target overexpression of ET-1 to the mouse endothelium, a TG was constructed by inserting the human preproET-1 coding sequence cDNA²⁵ into the endothelium-specific Tie-2 promoter/enhancer (plasmid pSPTg.T2FpAXK, a generous gift from Dr Tom Sato, University of Texas Southwestern Medical Center, Dallas). A portion of the mouse β -globin gene was incorporated into the TG immediately downstream of the ET-1 cDNA to provide an intron and a polyadenylation signal (Figure 1A). This promoter/enhancer combination has been shown to drive endothelium-specific expression of genes in TG mice.²⁴ Hybrid C3H \times C57BL/6 mouse embryos were microinjected with the plasmid according to standard protocols, and all subsequent breeding was carried out in the C57BL/6 line (Harlan Sprague-Dawley, Chicago, Ill). After microinjection, 72 live births were obtained, and from these births we obtained 4 lines but only 3 survived. Studies were confirmed by a second TG line to exclude possible genomic insertional effects of the TG. Genomic integration of the TG was confirmed on 3-week-old pup tail biopsy samples by polymerase chain reaction (PCR) with oligonucleotides specific for the TG (forward primer, 5'-AACACACTATTGCAATGAA-3' and reverse primer, 5'-ATGGATTATTTGCTCATGATT-3'). All animal protocols were conducted according to recommendations from

the Animal Care Committee of the Clinical Research Institute of Montreal and the Canadian Council of Animal Care.

Tissue Pattern of TG Expression

TG expression was confirmed by RNase protection assay (RPA) on total RNA for the TG and histone H4 (an internal control).²⁶ Labeled RNA probes were prepared from nucleotides 906 to 1763 of TG cDNA. For RPA, the Promega Riboprobe Gemini system (Promega) was used according to the manufacturer's protocol. In brief, 10 μ g total lung RNA isolated by the guanidinium thiocyanate-phenol-chloroform method was hybridized with a labeled RNA probe for the TG. Protected fragments fractionated on polyacrylamide-urea denaturing gels were then exposed to x-ray film. The protected fragment was 266 nucleotides long.

To confirm endothelial expression, aortas from TG mice were cut into 2 pieces, and the endothelium in the upper portion was gently removed with a stainless steel cannula, as described elsewhere with brief modifications.²⁷ Total RNA was extracted, and reverse transcription (RT)-PCR was carried out as previously described.²⁸ The sense primer used for TG detection was preproET-1 (5'-AAACAGCGTCAAATCATCTT-3'), whereas the antisense primer was that of rabbit β -globin (5'-AGACAGCACAATAACCAGCAC-3'). The presence of endothelium was confirmed by murine von Willebrand factor (vWF), an endothelium-specific marker (sense primer, 5'-GCGATTCCCACTCTTCC-3' and antisense primer, 5'-TTGACGAGGCAGGGGTTCC-3'). In addition, the sense primer for ribosomal protein S16, an internal control, was 5'-AGGAGCGATTGCTGGTGTGG-3', and the antisense primer was 5'-GCTACCAGGGCCTTTGAGATG-3'. The migration of each PCR product (148 bp, preproET-1- β -globin; 70 bp, vWF; 103 bp, S16) was detected on a 1.5% agarose gel and revealed after ethidium

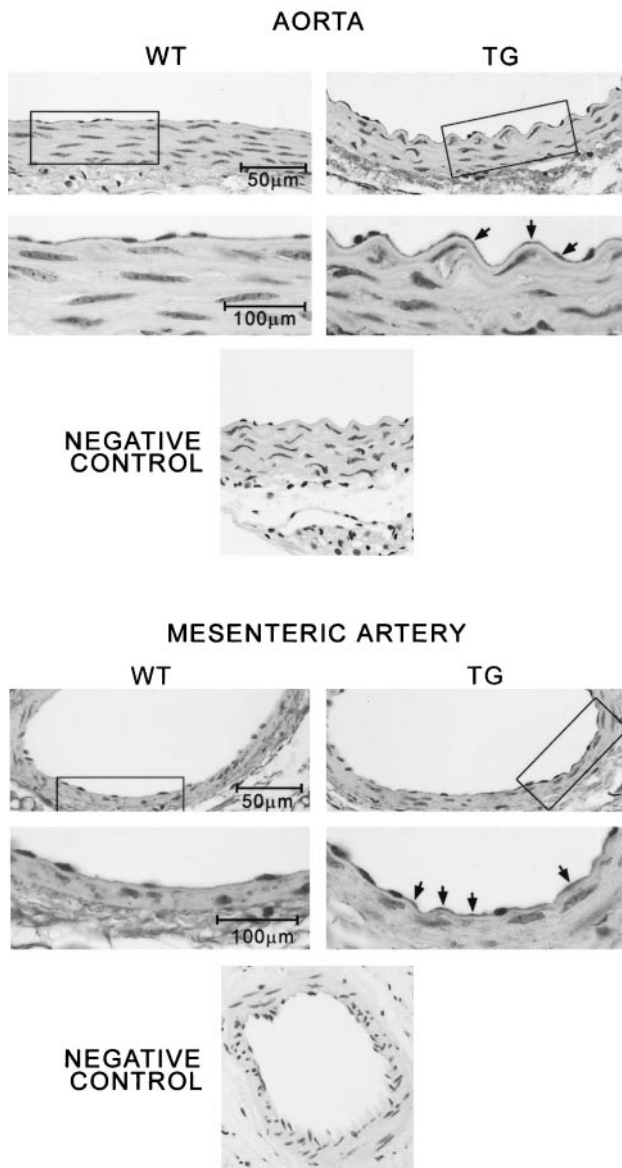


Figure 2. Immunohistochemical analysis of ET-1 in aortas and mesenteric vessels at low and high magnifications. Negative controls were incubated with nonimmune rabbit IgG instead of primary antibody. Arrows denote areas of intense staining in aortas and mesenteric arteries of TG mouse. Abbreviations are as defined in text.

bromide staining. To further confirm endothelial expression of the TG, *in situ* hybridization was carried out as previously described.²⁹

Quantification of ET-1, ET_A, and ET_B mRNA Expression

PreproET-1 mRNA levels were determined by quantitative PCR (qPCR). Primers for preproET-1 (human and murine) were sense, 5'-GCTGGTGGAGGGAAGAAAAC-3' and antisense, 5'-CACCA-CGGGGCTCTGTAGTC-3'; for murine ET_A, sense, 5'-TGTCTGC-TTCCGAGGAGC-3' and antisense, 5'-GTGCCAGAAAGTTGATC-3'; and for murine ET_B, sense, 5'-TAGGGCAGTTGACAACCT-3' and antisense, 5'-TCCTGTGAGAGTCTGGTAG-3'. qPCR for S16 was conducted as previously described.²⁸ Results are expressed as a ratio (relative quantities) between the gene of interest and S16.²⁸

Physiological Parameters of Animals and Morphological Characteristics of Vessels

Parameter	WT	TG
Body weight, g	22.9±0.7	21.4±0.5*
Tibia length (TL), cm	1.7±0.1	1.8±0.1
Heart weight (HW), mg	124.7±3.9	126.0±9.0
Left ventricle, mg	74.6±1.8	79.1±5.2
Right ventricle, mg	17.5±3.5	17.8±3.1
Kidney weight (KW), mg	149.6±6.2	138.8±4.7
HW/TL	72.9±2.3	74.7±4.8
KW/TL	87.4±3.7	82.6±3.6
Plasma ET-1 concentration, pg/mL	1.6±0.3	11.2±2.5†
Aorta		
Lumen diameter, μm	475.4±52.8	404.8±78.1
Media thickness, μm	80.2±5.3	81.5±5.5
Media/lumen	0.17±0.03	0.22±0.05
Medial CSA, ×10 ³ , μm	64.6±2.8	58.5±3.9
Mesenteric vessels		
Lumen diameter, μm	223.9±10.1	226.9±9.1
Media thickness, μm	11.5±0.5	14.9±1.1*
Media/lumen	4.8±0.2	6.5±0.6†
Medial CSA, ×10 ³ , μm	8.4±0.5	11.3±1.0*

Values are mean±SEM, n=6 mice per group. Abbreviations are as defined within Table or in text.

**P*<0.05 vs WT, †*P*<0.01 vs WT.

Immunohistochemistry

Immunohistochemistry was performed on aortas and mesenteric arteries as previously described.³⁰ In brief, paraffin-embedded, 5-μm sections were incubated with ET-1 antibody (1:100, Peninsula Laboratories) and then with a secondary conjugated IgG antibody (ABC kit, Vector Laboratories). The signal was revealed with 3,3'-diaminobenzidine (Sigma), and sections were counterstained with hematoxylin. The negative controls were incubated with non-immune rabbit IgG instead of the primary antibody.

Physiological Studies

Ten-week-old male TG and wild-type (WT) mice were surgically implanted with telemetric transmitters (TA11PA-C20, Data Sciences International), and systolic BP (SBP), diastolic BP (DBP), mean BP (MBP), and heart rate (HR) were measured as described elsewhere.³¹ Animals were allowed to recover for 7 days after surgery before baseline BP and HR data were collected. Hourly averages of 10-second samples obtained every 5 minutes were used to obtain values. Animals were then weighed and humanely killed; their hearts and kidneys were removed and weighed; and tibia length was measured.³² Aortas and mesenteric arteries were removed and fixed for histology or used for functional studies. Plasma ET-1 concentration was determined by an ELISA that detected specifically cleaved ET-1 (R&D Systems Inc).

Functional and Mechanical Studies

Second-order branches of the mesenteric arterial tree were dissected and placed in cold physiological salt solution (PSS) containing (in mmol/L) NaCl 120, NaHCO₃ 25, KCl 4.7, KH₂PO₄ 1.18, MgSO₄ 1.18, CaCl₂ 2.5, EDTA 0.026, and glucose 5.5. Vessels were mounted on a pressurized myograph as previously described.²⁸ Vessels were equilibrated (1 hour with PSS, bubbled with 95% air-5% CO₂, pH 7.4) at 37°C. Endothelium-dependent and -independent relaxations were assessed by measuring the dilatory responses to cumulative doses of acetylcholine (ACh, 10⁻⁹ to

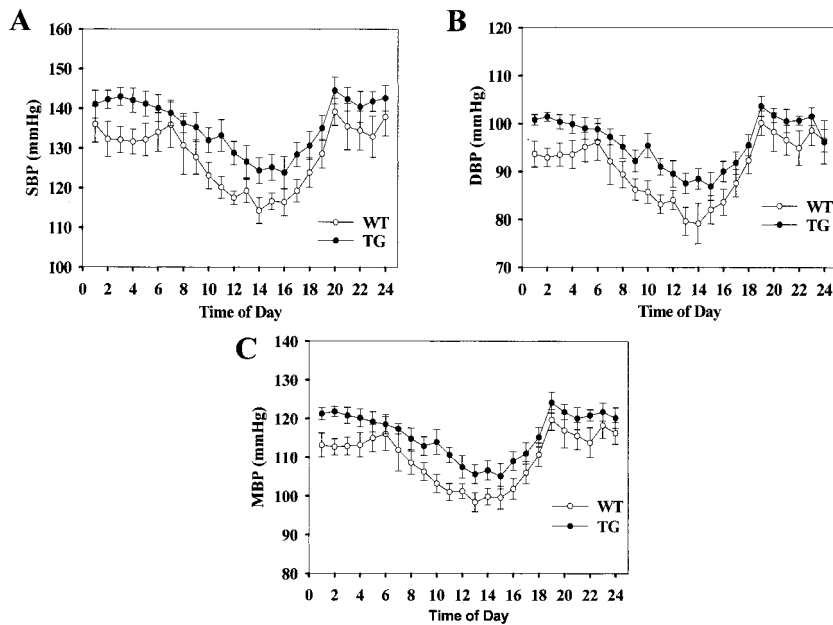


Figure 3. 24-Hour radiotelemetric analysis of hemodynamic parameters SBP (A), DBP (B), and MBP (C). Values are mean \pm SEM. Open and closed circles represent WT and TG mice, respectively. $n=6$ per group. Abbreviations are as defined in text.

10^{-4} mol/L) and sodium nitroprusside (10^{-8} to 10^{-4} mol/L), respectively, in vessels precontracted with norepinephrine (5×10^{-5} mol/L). Contractile responses were assessed by extraluminal perfusion with exogenous ET-1 (10^{-11} to 10^{-6} mol/L, Peninsula Laboratories) and norepinephrine (10^{-8} to 10^{-5} mol/L, Sigma). Vessels were assessed with and without endothelium denudation³³ in response to ET-1 and ET-3.

To evaluate nitric oxide (NO) bioavailability, in a different set of experiments the dose-response curve to Ach was determined before and after a 30-minute preincubation with the NO synthase inhibitor *N*^ω-nitro-L-arginine methyl ester (L-NAME, 100 μ mol/L, Sigma). To assess production of ROS, Ach administration was repeated in the presence of the antioxidants vitamin C and Tiron (100 μ mol/L and 100 mmol/L, respectively; 30-minute preincubations; Sigma). To evaluate whether oxidative stress could influence NO bioavailability, dose-response curves to Ach were repeated with simultaneous administration of L-NAME and vitamin C. To determine a possible source of ROS, dose-response curves to Ach were determined in the presence of apocynin, an NAD(P)H oxidase inhibitor.

Vessels were deactivated by perfusion with Ca^{2+} -free PSS containing 10 mmol/L EGTA for 30 minutes. Lumen and media were measured with intraluminal pressure at 45 mm Hg, and medial cross-sectional area (CSA) was evaluated as previously described.²⁸ The growth and remodeling indexes were calculated as described elsewhere.³⁴ Aortic media, lumen, and medial CSA measurements were quantified with the Northern Eclipse program (EMPIX Imaging Inc).

Measurement of NAD(P)H Oxidase Activity

Vascular NAD(P)H oxidase activity was measured by chemiluminescence with lucigenin and NADPH.³⁵

Western Blot Analysis

Aortic protein was extracted from frozen tissue³⁶ and separated by electrophoresis on polyacrylamide gels; transferred onto nitrocellulose membranes; and incubated with specific antibodies to ET_A, ET_B (Abcam), or gp91^{phox} (a gift from Dr Mark T. Quinn, Montana State University, Bozeman). Signals were revealed with chemiluminescence and visualized by autoradiography. Membranes were subsequently stripped (Pierce Biotechnology) and reprobbed with β -actin (Sigma) to verify equal loading. Optical density of the bands was quantified by AlphaEase software (Alpha Innotech Corp), normalized to that of β -actin, and expressed in arbitrary units.

Data Analysis

Results are presented as mean \pm SEM. Comparisons between groups were made by unpaired *t* test, ANOVA, or repeated-measures ANOVA, where appropriate. The area under the curve (AUC) was calculated for dose-response curves with GraphPad software. A value of $P < 0.05$ was considered statistically significant.

Results

TG Expression

RPA with lung tissue (rich in endothelial cells) demonstrated expression of the human preproET-1–coding TG under Tie-2 promoter control in TG but not in WT mice (Figure 1B). RT-PCR showed TG expression to be specifically targeted to the endothelium, because both the TG and vWF were virtually absent in denuded aortas but were present in aortas with intact endothelium (Figure 1C). These findings were confirmed in lung tissues by in situ hybridization (Figure 1D).

PreproET-1 mRNA Quantification and ET-1 Localization

A 3-fold increase in aortic preproET-1 mRNA in TG mice compared with WT littermates was demonstrated by qPCR (0.76 ± 0.04 versus 0.26 ± 0.11 , $P < 0.01$, $n=6$). In TG mice, vascular ET-1 immunostaining was noted in the endothelium compared with WT mice (Figure 2).

Physiological Parameters

TG mice exhibited a 7-fold increase in plasma ET-1 levels compared with WT littermates (Table). These data, taken together with the tissue preproET-1 mRNA and ET-1 expression findings, suggest that in these TG mice, there was constitutive secretion of ET-1.

Although TG mice had a slightly lower body weight but no change in tibia length, and kidney and heart weights were comparable to those of WT littermates, no significant differences were observed in either heart weight–tibia length or kidney weight–tibia length ratios, indicating the absence of

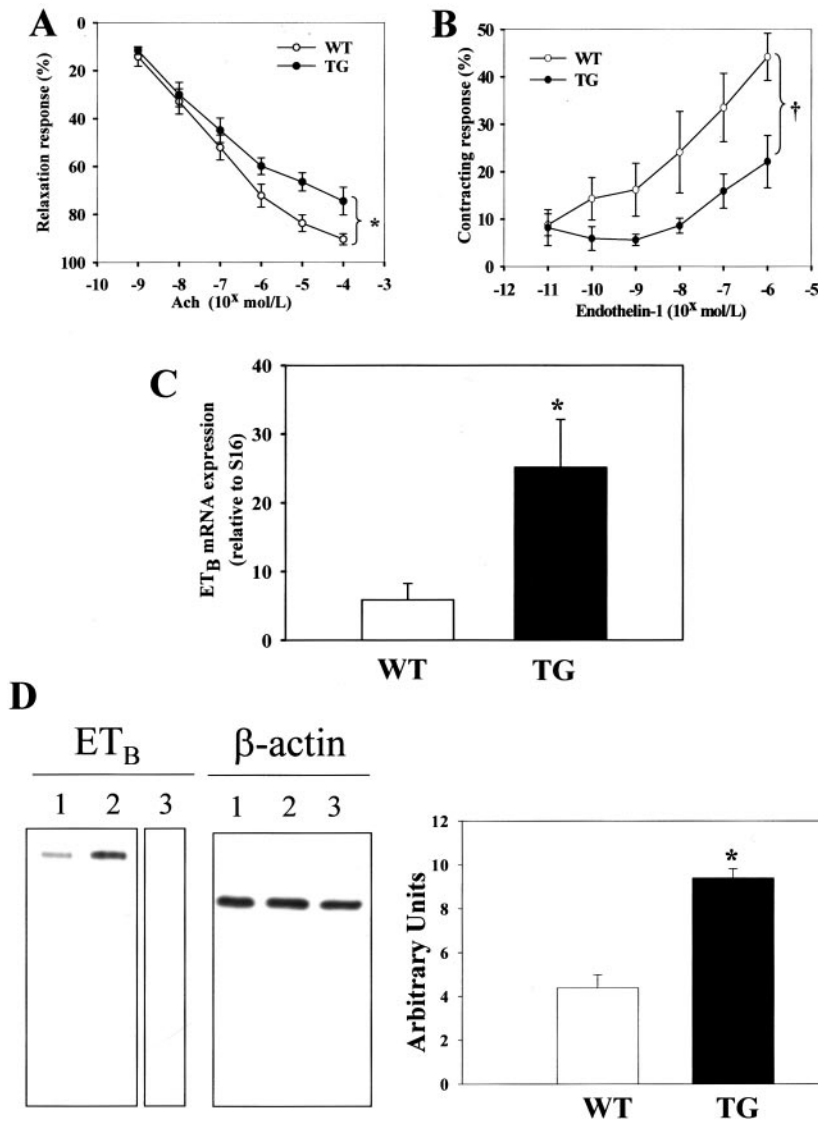


Figure 4. Resistance artery endothelial function and response to exogenous ET-1. Concentration-response curves for Ach (A) and ET-1 (B). Relaxation responses are percent increase in lumen after norepinephrine precontraction. Contractile response is percent reduction in lumen. Vascular ET receptor quantification: ET_B mRNA (C) and ET_B protein (D). Left, Representative blots of ET_B and β -actin: lane 1, WT; lane 2, TG; lane 3: TG without ET_B antibody. Right, Values are mean \pm SEM. Open and closed symbols represent WT and TG mice, respectively. $n=6$, * $P<0.05$, † $P<0.01$. Abbreviations are as defined in text.

hypertrophy in these organs (Table). In addition, no significant differences in HR between groups were detected (not shown). TG mice showed a trend toward a slight elevation in SBP, DBP, and MBP throughout the 24-hour daily cycle compared with WT littermates. However, these differences were small, and although they were constant throughout the 24-hour daily cycle, they did not reach statistical significance (Figure 3).

Morphology of Conduit and Resistance Vessels

TG mice exhibited increased media thickness of mesenteric resistance arteries (Table) with a significantly increased media-lumen ratio and medial CSA (Table) and a growth index of 34% compared with age-matched WT animals. However, no differences in aortic medial CSA and media-lumen ratio were observed between WT and TG mice (Table).

Endothelial Function of Resistance Arteries

Vasodilation of resistance arteries was significantly attenuated in TG mice compared with WT mice (Figure 4A; AUC, 293.2 ± 21.1 versus 244.2 ± 17.5 , respectively; $P<0.05$), whereas endothelium-independent relaxation by sodium ni-

troprusside was similar in both groups (not shown). Although no difference in contractile responses to norepinephrine was observed (not shown), TG mice exhibited blunted vasoconstrictor responses to ET-1 compared with WT mice (Figure 4B; AUC, 134.0 ± 30.9 versus 51.2 ± 12.8 , respectively; $P<0.01$) and an increased response to ET-3 in vessels with an intact endothelium (AUC, 114.0 ± 29.7 versus 186.2 ± 58.7 , respectively; $P<0.05$). When the endothelium was removed, ET-3 vasoconstrictor responses were similar between TG and WT mice (not shown).

To elucidate potential mechanisms underlying the ET-1 and ET-3 altered responses in TG mice, we evaluated vascular ET_A and ET_B receptor mRNA and protein levels. No differences were observed in ET_A mRNA and protein levels between groups (not shown). However, there was a significant ($P<0.05$) increase in ET_B mRNA and protein levels (Figure 4C and 4D) in TG mice.

Role of ROS in Endothelial Dysfunction

In TG mice, the inhibitory effect of L-NAME on Ach (AUC Ach, 244.2 ± 17.5 ; with L-NAME, 174.1 ± 31.0 ; inhibition of

27.4±10.7) was significantly lower, as indicated by a higher AUC, than in WT mice (AUC Ach, 311.9±12.8; with L-NAME, 130.2±19.0; inhibition of 50.3±6.9; Figure 5). In TG mice, vitamin C restored responses to Ach (AUC, 276.3±30.3) and the inhibitory effects of L-NAME (195.7±37.6; inhibition, 21.7±15.1; Figure 5B and 5C). In WT littermates, the antioxidant failed to modify the effect of Ach (AUC, 292.1±21.3) or its inhibition by L-NAME (AUC, 118.5±12.2; inhibition, 58.9±4.4; Figure 5B and 5C). In the presence of vitamin C, relaxation by Ach and inhibition by L-NAME were not different in TG and WT mice (AUC, 118.5±12.2 versus 163.0±43.8, respectively; Figure 5C). Similar results were obtained with Tiron (not shown). Moreover, in TG mice, apocynin restored responses to Ach similar to those observed in WT animals (AUC, 304.4±9.1 versus 350.8±26.1, respectively).

NAD(P)H oxidase activity in TG mice was significantly increased ($P<0.05$) in both mesenteric (Figure 6A) and aortic vessels (not shown) compared with that in the WT counterparts. gp91^{phox}, a subunit of NAD(P)H oxidase, was also significantly increased in TG mice (Figure 6B).

Discussion

ET-1 plays a major role in abnormal vascular function and remodeling of resistance arteries in cardiovascular disease. However, to date there have been no experimental models in which the source of ET-1 overproduction originated uniquely from the endothelium and not from adjacent smooth muscle cells or other tissues.

Contrary to previous human preproET-1 TG animals in which the human preproET-1 gene was placed under the control of the murine preproET-1 promoter,^{13,14} we successfully targeted the TG containing the human preproET-1 specifically to the endothelium by using promoter/enhancer regions of the endothelium-specific tyrosine kinase receptor Tie-2. The present study provides the first unambiguous *in vivo* demonstration that endothelium-restricted ET-1 overexpression leads to altered vascular structure and function in the absence of a significant elevation of BP. The importance of these findings is that we may distinguish unequivocally between BP-dependent and -independent effects of endothelium-generated ET-1 on vascular remodeling and endothelial function in resistance vessels. We observed no deleterious end-organ damage attributable to BP elevation, as demonstrated by the absence of cardiac hypertrophy. This agrees with the absence of cardiac hypertrophy despite the development of ET-1-dependent cardiac fibrosis in other experimental models of hypertension, in which ET-1 production was elevated in the vasculature.³⁷

It may appear surprising that although DOCA-salt^{15,16} and Dahl salt-sensitive rats,²¹ which overexpress vascular ET-1, have elevated BP that can be lowered by ET antagonists, BP was not significantly elevated in our TG model overexpressing ET-1. BP elevation is the result of complex interactions between different factors that include ET-1 and kidney damage, the sympathetic system, and vasopressin activation in these models,^{5,6} which may not be present in ET-1 TG mice. In these models, the overexpression of ET-1 is not restricted to the endothelium, in contrast to the present TG

model. Thus, although ET-1 may induce vascular damage, by itself this may not significantly raise BP. There was a very small but not statistically significant difference in SBP, DBP, and MBP throughout the 24 hours of telemetrically recorded BP. This inability to induce a hypertensive effect has also been shown by an absence of BP elevation after ET-1 infusion³⁸ but may change in other experimental paradigms, such as after salt loading. Other peptides such as angiotensin II may not only induce vascular remodeling and endothelial dysfunction^{17,20} but also trigger complex renal and sympathetic nervous system responses of sufficient magnitude that,

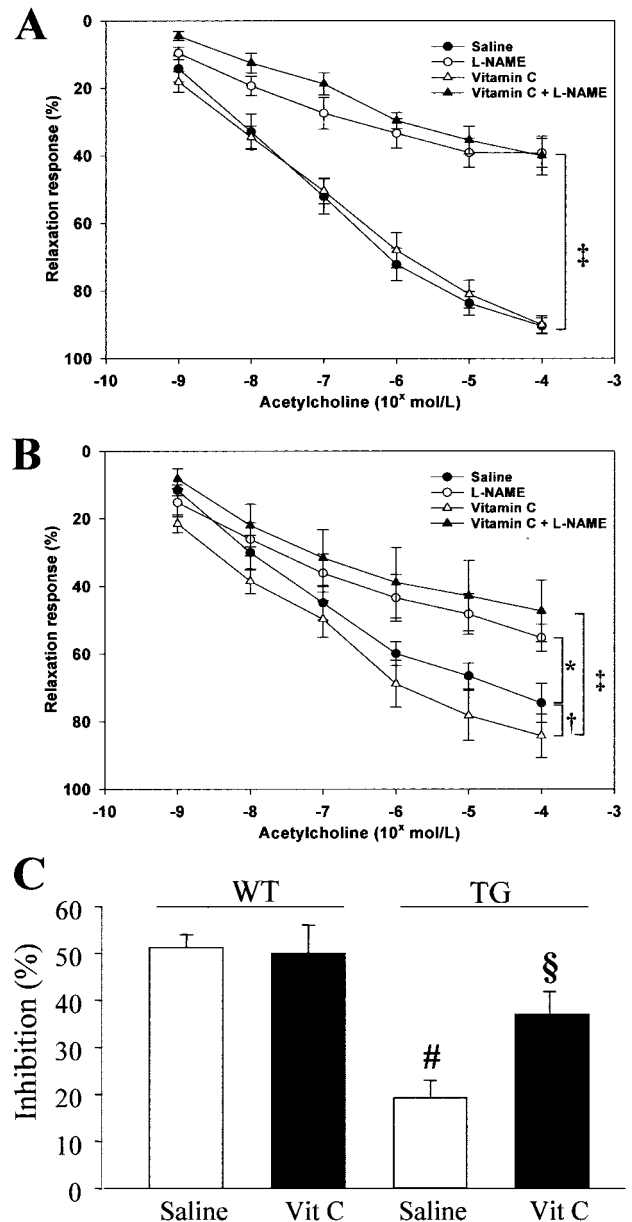


Figure 5. Endothelium-dependent relaxation of mesenteric resistance arteries from WT (A) and TG (B) mice to Ach in absence (saline, filled circles) and presence of L-NAME (open circles), vitamin C (open triangles), or both (filled triangles). C, Inhibition exerted by L-NAME on maximal relaxation response of mesenteric resistance arteries from WT and TG mice. Values are mean±SEM, n=6. * $P<0.05$, † $P<0.01$, ‡ $P<0.001$, # $P<0.001$ vs WT saline; § $P<0.05$ vs WT saline and TG saline.

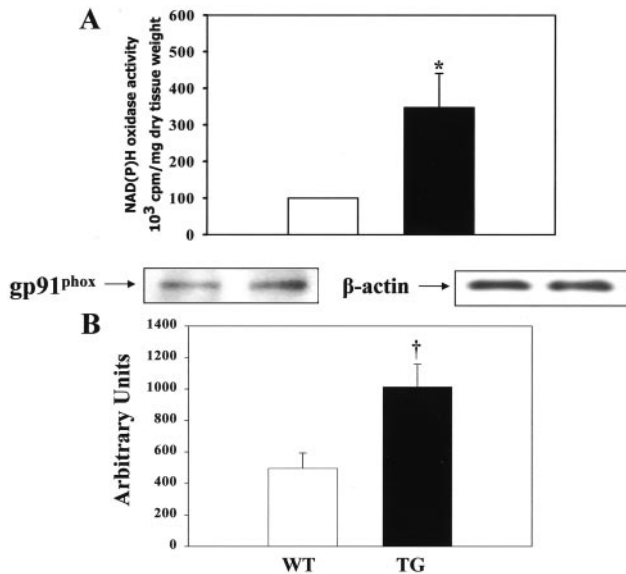


Figure 6. Vascular NADPH oxidase activity in mesenteric arteries (A) of WT and TG mice. B, top, Representative Western blot of gp91^{phox} and β -actin. Bottom, Values are mean \pm SEM. Open and closed symbols represent WT and TG mice, respectively. n=6, * P <0.01, † P <0.05.

together with vascular damage, result in hypertension. Despite the lack of a significant effect on BP, enhanced endothelial ET-1 in TG mice had the ability to directly induce significant hypertrophic remodeling in resistance vessels, as demonstrated by an increased media-lumen ratio and medial CSA and a growth index of 34% in resistance arteries that cannot be explained by hemodynamic factors. TG mice exhibited altered vascular responses to ET-1 and ET-3, which were normalized in endothelium-denuded vessels. These events, together with the increased ET_B expression, may be responsible for the altered vascular responses to ET-1 and ET-3.

TG mice exhibited impaired endothelium-dependent relaxation, which may be attributed to antagonism between the overexpressed endothelial human ET-1 and endothelium-derived NO.³⁹ To investigate possible mechanisms responsible for endothelial dysfunction, NO bioavailability and oxidative stress were assessed by using the NOS inhibitor L-NAME and the antioxidants vitamin C and Tiron. In WT mice, vasodilation to Ach was significantly reduced by L-NAME. Vitamin C and Tiron failed to modify the response to Ach or the inhibitory effect of L-NAME, indicating that, as expected under normal conditions, NO bioavailability was preserved and oxidant excess was absent. In TG animals the inhibitory effect of L-NAME on Ach, though present, was reduced compared with that in WT, suggesting reduced NO availability. Antioxidants improved relaxation to Ach, indicating the participation of ROS in endothelial dysfunction in these mice, and restored the inhibitory effects of L-NAME, as NO bioavailability was increased by the antioxidant. Thus, in TG mice overexpressing human ET-1, reduced NO resulted from increased ROS production, which agrees with previous studies proposing a role for ROS in the mechanisms responsible for ET-1-induced endothelial dysfunction.^{40,41}

A possible source of the increased ROS generation in TG mice could be the enzyme NAD(P)H oxidase.^{17,22,42} This concept is supported by the increase in vascular NAD(P)H oxidase activity and gp91^{phox} subunit expression, as well as the relaxation restored by Ach after pretreatment with apocynin in TG mice. ET-1 is known to be preferentially secreted abluminally.³ In the present model, ET-1 overexpressed only in the endothelium may be secreted toward underlying smooth muscle cells to induce growth and extracellular matrix deposition, resulting in structural remodeling of small arteries. In the endothelium, where the TG was overexpressed and ET-1 concentration was presumably highest, it will result in increased formation of ROS²⁸ and decreased bioavailability of NO and endothelial dysfunction.⁴³

Conclusion

We have demonstrated with a TG approach that endothelium-secreted, human ET-1 induces vascular remodeling and endothelial dysfunction in mice in the absence of significant increases in BP. ET-1 may induce resistance-artery remodeling directly, as we previously suggested on the basis of less compelling data.^{1,15} These results underscore the importance of pursuing attempts to develop agents that can be used in humans to block the ET system to reduce the complications of high BP and the burden of cardiovascular disease.

Acknowledgments

This work was supported by grant 37917 (to Dr Schiffrin) and a group grant to the Multidisciplinary Research Group on Hypertension, both from the Canadian Institutes of Health Research (CIHR). We are grateful to Chantal Mercure, André Turgeon, Laura Davis, Jadwiga Marcinkiewicz, Manon Laprise, and Qinzhang Zhu for their excellent technical assistance.

References

- Schiffrin EL. Endothelin: potential role in hypertension and vascular hypertrophy. *Hypertension*. 1995;25:1135–1143.
- Yanagisawa M, Kurihara H, Kimura S, et al. A novel potent vasoconstrictor peptide produced by vascular endothelial cells. *Nature*. 1988;332:411–415.
- Wagner OF, Christ G, Wojta J, et al. Polar secretion of endothelin-1 by cultured endothelial cells. *J Biol Chem*. 1992;267:16066–16068.
- Miyauchi T, Masaki T. Pathophysiology of endothelin in the cardiovascular system. *Annu Rev Physiol*. 1999;61:391–415.
- Schiffrin EL. Role of endothelin-1 in hypertension and vascular disease. *Am J Hypertens*. 2001;14:83S–89S.
- Kurihara Y, Kurihara H, Suzuki H, et al. Elevated blood pressure and craniofacial abnormalities in mice deficient in endothelin-1. *Nature*. 1994;368:703–710.
- Berthiaume N, Yanagisawa M, Yanagisawa H, et al. Pharmacology of endothelins in vascular circuits of normal or heterozygous endothelin-A or endothelin-B knockout transgenic mice. *J Cardiovasc Pharmacol*. 1998;31(suppl 1):S561–S564.
- Hosoda K, Hammer RE, Richardson JA, et al. Targeted and natural (piebald-lethal) mutations of endothelin-B receptor gene produce megacolon associated with spotted coat color in mice. *Cell*. 1994;79:1267–1276.
- Puffenberger EG, Hosoda K, Washington SS, et al. A missense mutation of the endothelin-B receptor gene in multigenic Hirschsprung's disease. *Cell*. 1994;79:1257–1266.
- Yanagisawa H, Yanagisawa M, Kapur RP, et al. Dual genetic pathways of endothelin-mediated intercellular signaling revealed by targeted disruption of endothelin converting enzyme-1 gene. *Development*. 1998;125:825–836.
- Yanagisawa H, Hammer RE, Richardson JA, et al. Disruption of ECE-1 and ECE-2 reveals a role for endothelin-converting enzyme-2 in murine cardiac development. *J Clin Invest*. 2000;105:1373–1382.

12. Hocher B, Thone-Reineke C, Rohmeiss P, et al. Endothelin-1 transgenic mice develop glomerulosclerosis, interstitial fibrosis, and renal cysts but not hypertension. *J Clin Invest*. 1997;99:1380–1389.
13. Shindo T, Kurihara H, Maemura K, et al. Renal damage and salt-dependent hypertension in aged transgenic mice overexpressing endothelin-1. *J Mol Med*. 2002;80:105–116.
14. Li JS, Larivière R, Schiffrin EL. Effect of nonselective endothelin antagonist on vascular remodeling in DOCA-salt hypertensive rats: evidence for a role of endothelin in vascular hypertrophy. *Hypertension*. 1994;24:183–188.
15. Schiffrin EL, Larivière R, Li JS, et al. Deoxycorticosterone acetate plus salt induces overexpression of vascular endothelin-1 and severe vascular hypertrophy in spontaneously hypertensive rats. *Hypertension*. 1995;25:769–773.
16. Duerrschmidt N, Wippich N, Goettsch W, et al. Endothelin-1 induces NAD(P)H oxidase in human endothelial cells. *Biochem Biophys Res Commun*. 2000;269:713–717.
17. Li L, Fink GD, Watts SW, et al. Endothelin-1 increases vascular superoxide via endothelin A–NADPH oxidase pathway in low-renin hypertension. *Circulation*. 2003;107:1053–1058.
18. Intengan HD, Schiffrin EL. Structure and mechanical properties of resistance arteries in hypertension. *Hypertension*. 2000;36:312–318.
19. Mulvany MJ, Baumbach GL, Aalkjaer C, et al. Vascular remodeling. *Hypertension*. 1996;28:505–506.
20. Intengan HD, Schiffrin EL. Vascular remodeling in hypertension: roles of apoptosis and fibrosis. *Hypertension*. 2001;38:581–587.
21. d'Uscio LV, Barton M, Shaw S, et al. Structure and function of small arteries in salt-induced hypertension: effects of chronic endothelin-subtype-A-receptor blockade. *Hypertension*. 1997;30:905–911.
22. Li L, Watts SW, Banas AK, et al. NADPH oxidase-derived superoxide augments endothelin-1-induced vasoconstriction in mineralocorticoid hypertension. *Hypertension*. 2003;42:316–321.
23. Cai H, Griendling KK, Harrison DG. The vascular NAD(P)H oxidases as therapeutic targets in cardiovascular diseases. *Trends Pharmacol Sci*. 2003;24:471–478.
24. Schlaeger TM, Bartunkova S, Lawitts JA, et al. Uniform vascular-endothelial-cell-specific gene expression in both embryonic and adult transgenic mice. *Proc Natl Acad Sci U S A*. 1997;94:3058–3063.
25. Itoh Y, Yanagisawa M, Ohkubo S, et al. Cloning and sequence analysis of cDNA encoding the precursor of a human endothelium-derived vasoconstrictor peptide, endothelin: identity of human and porcine endothelin. *FEBS Lett*. 1988;231:440–444.
26. Lochard N, Silversides DW, van Kats JP, et al. Brain-specific restoration of angiotensin II corrects renal defects seen in angiotensinogen-deficient mice. *J Biol Chem*. 2003;278:2184–2189.
27. Miller AL, Plane F, Jeremy JY, et al. Delayed recovery of receptor-mediated functional responses to Ach in mouse isolated carotid arteries following endothelial denudation in vivo. *J Vasc Res*. 2003;40:449–459.
28. Iglarz M, Touyz RM, Amiri F, et al. Effect of peroxisome proliferator-activated receptor- α and - γ activators on vascular remodeling in endothelin-dependent hypertension. *Arterioscler Thromb Vasc Biol*. 2003;23:45–51.
29. Day R, Larivière R, Schiffrin EL. *In situ* hybridization shows increased endothelin-1 mRNA levels in endothelial cells of blood vessels of deoxycorticosterone acetate-salt hypertensive rats. *Am J Hypertens*. 1995;8:294–300.
30. Schiffrin EL, Larivière R, Li JS, et al. Enhanced expression of the endothelin-1 gene in blood vessels of DOCA-salt hypertensive rats: correlation with vascular structure. *J Vasc Res*. 1996;33:235–248.
31. Carlson SH, Wyss JM. Long-term telemetric recording of arterial pressure and heart rate in mice fed basal and high NaCl diets. *Hypertension*. 2000;35:1e–5e.
32. Yin FC, Spurgeon HA, Rakusan K, et al. Use of tibial length to quantify cardiac hypertrophy: application in the aging rat. *Am J Physiol*. 1982;243:H941–H947.
33. Miller AL, Plane F, Jeremy JY, et al. Delayed recovery of receptor-mediated functional responses to acetylcholine in mouse isolated carotid arteries following endothelial denudation in vivo. *J Vasc Res*. 2003;40:449–59.
34. Heagerty AM, Aalkjaer C, Bund SJ, et al. Small artery structure in hypertension: dual process of remodeling and growth. *Hypertension*. 1993;21:391–397.
35. Virdis A, Iglarz M, Neves MF, et al. Effect of hyperhomocystinemia and hypertension on endothelial function in methylenetetrahydrofolate reductase-deficient mice. *Arterioscler Thromb Vasc Biol*. 2003;23:1352–1357.
36. Diep QN, El Mabrouk M, Cohn JS et al. Structure, endothelial function, cell growth and inflammation in blood vessels of angiotensin II-infused rats: role of peroxisome proliferator-activated receptor- γ . *Circulation*. 2002;105:2296–2302.
37. Ammarguella F, Larouche I, Schiffrin EL. Myocardial fibrosis in DOCA-salt hypertensive rats: effect of endothelin ET_A receptor antagonism. *Circulation*. 2001;103:319–324.
38. Mortensen LH, Fink GD. Salt-dependency of endothelin-induced, chronic hypertension in conscious rats. *Hypertension*. 1992;19:549–554.
39. Chatziantoniou C, Boffa JJ, Ardaillou R, et al. Nitric oxide inhibition induces early activation of type I collagen gene in renal resistance vessels and glomeruli in transgenic mice: role of endothelin. *J Clin Invest*. 1998;101:2780–2789.
40. Wedgwood S, Dettman RW, Black SM. ET-1 stimulates pulmonary arterial smooth muscle cell proliferation via induction of reactive oxygen species. *Am J Physiol*. 2001;281:L1058–L1067.
41. Park JB, Touyz RM, Chen X, et al. Chronic treatment with a superoxide dismutase mimetic prevents vascular remodeling and progression of hypertension in salt-loaded stroke-prone spontaneously hypertensive rats. *Am J Hypertens*. 2002;15:78–84.
42. Sedeek MH, Llinas MT, Drummond H, et al. Role of reactive oxygen species in endothelin-induced hypertension. *Hypertension*. 2003;42:806–810.
43. Tomasian D, Keaney JF, Vita JA. Antioxidants and the bioactivity of endothelium-derived nitric oxide. *Cardiovasc Res*. 2000;47:426–435.

Endothelium-Restricted Overexpression of Human Endothelin-1 Causes Vascular Remodeling and Endothelial Dysfunction

Farhad Amiri, Agostino Virdis, Mario Fritsch Neves, Marc Iglarz, Nabil G. Seidah, Rhian M. Touyz, Timothy L. Reudelhuber and Ernesto L. Schiffrin

Circulation. 2004;110:2233-2240; originally published online October 4, 2004;
doi: 10.1161/01.CIR.0000144462.08345.B9

Circulation is published by the American Heart Association, 7272 Greenville Avenue, Dallas, TX 75231
Copyright © 2004 American Heart Association, Inc. All rights reserved.
Print ISSN: 0009-7322. Online ISSN: 1524-4539

The online version of this article, along with updated information and services, is located on the
World Wide Web at:

<http://circ.ahajournals.org/content/110/15/2233>

Permissions: Requests for permissions to reproduce figures, tables, or portions of articles originally published in *Circulation* can be obtained via RightsLink, a service of the Copyright Clearance Center, not the Editorial Office. Once the online version of the published article for which permission is being requested is located, click Request Permissions in the middle column of the Web page under Services. Further information about this process is available in the [Permissions and Rights Question and Answer](#) document.

Reprints: Information about reprints can be found online at:
<http://www.lww.com/reprints>

Subscriptions: Information about subscribing to *Circulation* is online at:
<http://circ.ahajournals.org/subscriptions/>